ISBN: 978-3-95450-184-7 doi:10.18429/JACoW-IPAC2018-THPAK137

BEAM-BASED SEXTUPOLAR NONLINEARITY MAPPING IN CESR*

L. Gupta†, S. S. Baturin, Y.-K. Kim University of Chicago, Chicago, IL, USA
J. M. Maxson, M. Ehrlichman, R. Meller, D. Rubin, D. Sagan, J. Shanks,
Cornell University, Ithaca, NY, USA

Abstract

In order to maintain beam quality during transport through a storage ring, sextupole magnets are used to make chromatic corrections, but necessarily introduce deleterious effects such as nonlinear resonances and reduced dynamic aperture. Implementing intricate sextupole distributions to mitigate these effects will rely on precision beam-based measurement of the applied sextupole distribution. In this work, we generalize previous sextupole mapping techniques by using resonant phase-locked excitation of the beam at the Cornell Electron Storage Ring (CESR) [1], which accounts for variations in the normal mode tunes on a turn by turn basis. The methods presented here are applied to simulation and actual turn by turn (TbT) data in CESR for both simplified and realistic sextupole distributions.

INTRODUCTION

Progress toward lower emittance in storage ring synchrotron light sources to achieve diffraction limited beam quality at angstrom wavelengths will necessarily require stronger chromaticity correction [2], and thus the online diagnosis and correction of storage ring sextupole distributions may become an important tool in the preservation and maximization of dynamic aperture.

Methods for locating and measuring the magnitude of sextupole field errors have been demonstrated with good success by using TbT BPM measurements [3, 4]. These methods employ a spectral analysis of BPM data for the calculation of resonant driving terms (RDTs) that encode sextupole field error information [5]. Coherent displacement of the beam is either performed with a single pulsed kicker (pinger) or an ac dipole. In the case of a pinged beam, the number of useful turns in the analysis is limited by radiation damping. The ac dipole technique can accumulate many more turns of TbT data [6], in CESR, tune trackers are used to synchronously drive the beam at the betatron tunes (in both planes) even in the presence of phase jitter arising from guide field fluctuations on time scales of ~100 turns [7]. This configuration serves as an ideal test-bed for a robust sextupole field error mapping method to be developed.The current progress for this project including successful sextupole field error location and measurement in simulation, and and progress toward the same in experiment are presented.

* Work supported by NSF Award No. PHY-1549132 (Center for Bright Beams)
† lipigupta@uchicago.edu

SIMPLE MODEL OF BEAM RESPONSE

To develop the mathematical model for determining how turn-by-turn BPM measurements can be analyzed to measure sextupole field errors in the presence of turn by turn tune jitter, a simplified model (as compared to full RDT analysis) of the spectral response to beam shaking was developed.

We start by considering a simplified nearly-linear CESR lattice with a single sextupole with gradient k_2 and length L. Thus the angular kick in the x-direction is $\delta\theta_x = \frac{K}{2}(x_S^2 + y_S^2)$, where x_S and y_S are the spatial coordinates of the centroid of the beam in the sextupole, and $K = k_2 L$. We define the unperturbed oscillations at the sexutpole to have the form

$$x_S(t) = \sqrt{2A_x\beta_{x,S}}\cos(\omega_x t), \tag{1}$$

for action A_x and horizontal beta function at the sextupole, $\beta_{x,S}$. Then, we compute δx_B, the linear order change in the x position at a beam position monitor by summing the angular kicks exerted on the beam at each turn:

$$\begin{aligned}\delta x_B(t) \quad = \quad & \delta\theta(t)\sqrt{\beta_{x,B}\beta_{x,S}}\sin(\Delta\phi_{S\to B}) + \\ & \delta\theta(t-1)\sqrt{\beta_{x,B}\beta_{x,S}}\sin(\omega_x + \Delta\phi_{S\to B}) + \\ & \delta\theta(t-2)\sqrt{\beta_{x,B}\beta_{x,S}}\sin(2\omega_x + \Delta\phi_{S\to B}) + \ldots,\end{aligned}$$

given the beta functions $\beta_{x,B}$ and $\beta_{x,S}$ at the BPM and sextupole respectively,the betatron phase advance between the sextupole and the BPM $\Delta\phi_{S\to B}$, and ω_x, the one turn phase advance. The sum, written compactly, is

$$\delta x_B(t) = \sum_{k=0}^{\infty}\delta\theta(t-k)\sqrt{\beta_{x,B}\beta_{x,S}}\sin(k\omega_x + \Delta\phi_{S\to B}), \tag{2}$$

and has a closed form solution, but is omitted here for compactness. After computing this sum, the Fourier transform of the beam's response at the BPM is performed to determine the magnitude of the resonant tune line in frequency-space. The horizontal response will contain resonances at $2Q_x$ and $2Q_y$, while the vertical direction has resonant lines at $Q_x \pm Q_y$. The computed magnitudes $|\widetilde{C}_{2\omega_x}|$ and $|\widetilde{C}_{\omega_x+\omega_y}|$ are linearly proportional to K. Therefore, in order to determine the magnitude of K, resonance amplitude measurements can be fit by this model. Note that this analysis is trivially extended to the case in which the tune varies on each turn, replacing ω_x with the instantaneous tune on a given turn k, $\omega_{x,k}$. The tune tracker system at CESR reports this phase each turn, and thus may be directly incorporated in the model.

SIMULATION RESULTS

The above model was applied to simulated BPM measurements for a CESR lattice with a single, strong sextupole.

ISBN: 978-3-95450-184-7 doi:10.18429/JACoW-IPAC2018-THPAK137

The simulations were run using the Bmad charged particle subroutine library [8], in which the beam is displaced horizontally and vertically by 0.5mm in the absence of radiation damping, then tracked for 10,000 turns. In order generate sufficient signal in the betatron harmonics, the single sextupole was set at four times its nominal strength, thus overwhelming the extraneous signals from other nonlinearities in the ring. Alternatively, given the linearity of the above model, the zero-sextupole harmonic response could otherwise be removed as a baseline from the complex response of the beam at a given harmonic [5].

The simulated data was processed by taking the Fourier transform at each BPM and recording the $2Q_x$ harmonic line amplitudes, $|\widetilde{Q}_{2\omega_x}|$ from the horizontal spatial data, and $|\widetilde{Q}_{\omega_x+\omega_y}|$ from the vertical data. In order to fit the data to the model the following merit function was constructed:

$$\chi^2 = \sum^{N} \frac{(|\widetilde{C}_{2\omega_x}|-|\widetilde{Q}_{2\omega_x}|)^2}{\max((|\widetilde{C}_{2\omega_x}|-|\widetilde{Q}_{2\omega_x}|)^2)} + \frac{(|\widetilde{C}_{\omega_x+\omega_y}|-|\widetilde{Q}_{\omega_x+\omega_y}|)^2}{\max((|\widetilde{C}_{\omega_x+\omega_y}|-|\widetilde{Q}_{\omega_x+\omega_y}|)^2)} \tag{3}$$

A simple fitting routine was used to minimize Eq. 3, by varying the amplitude and phase of the spectral line. The fitted Fourier amplitudes for the simulation are shown in Fig. 1 and Fig. 2.

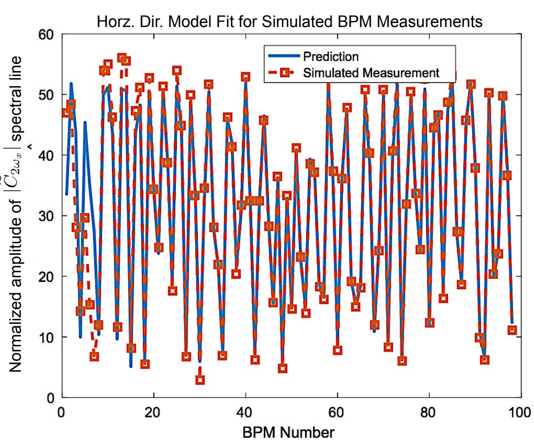

Figure 1: Comparison of $|\widetilde{C}_{2\omega_x}|$ spectral line amplitudes at each BPM between simulated BPM measurements and amplitudes calculated from the fitted model, in order to determine the field gradient k_2 and location of the single sextupole magnet.

The fitted model predicted that the sextupole was located at 40.6431m from the beginning of the lattice, and had $K = 1.0381\text{m}^{-2}$. After fitting, the model located the end of the sextupole accurately. The correct simulation setting for K was $K = 1.0336\text{m}^{-2}$, thus the sextupole field gradient was determined to within 0.5%. It will be important to understand both in simulation and experiment the noise to signal ratio, and what level of accuracy can be achieved consistently.

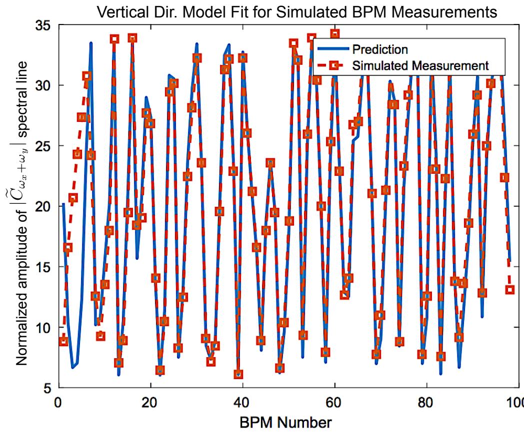

Figure 2: Comparison of $|\widetilde{C}_{\omega_x+\omega_y}|$ spectral line amplitudes at each BPM between simulated BPM measurements and amplitudes calculated from the fitted model, in order to determine the field gradient k_2 and location of the single sextupole magnet.

CURRENT EXPERIMENTAL PROGRESS

TbT measurement comparable to the simulated data were collected durin CESR machine studies in March 2018. During these experiments, the beam is resonantly driven by vertical and horizontal tune trackers and BPM data was acquired on a TbT basis using the CBPM system [9]. The tune trackers were driven maximally without incurring beam scraping, in order to maximize the resonant signals in the BPM measurement spectra. Further, unlike the simulation, CESR was configured to have a 2-family sextupole distribtuion, starting with chromaticity compensated to near zero. The field gradient at a single sextupole was doubled until the maximum strength was reached. These measurements were repeated for two different sextupoles in the lattice.

Equation 3 can be applied to this data as well as simple spectral analysis tools. An example spectrum is shown in Fig. 3. It is useful to remove the baseline signal in order to study changes in the signal which reflect nonlinearities such as sextupole field errors. Following Ref. [5], the nominal machine setting signal was subtracted from the signals measured with a given sextupole was increased in field strength. From these signals the horizontal and fundamental second harmonic phase advance were calculated, and a discontinuity was observed in both, near the known location of the sextupole. The discontinuity in the betatron phase advance is caused by a quadrupole error due arising from nonzero orbit in the sextupole, and is not unexpected. However, additional discontinuities are observed in the phase of the second harmonic tune line beyond that generated at the position of the sextupole, and thus in the current analysis this phase was not predictive in the determining the location of the sextupole. Work is ongoing to determine and mitigate the source of extraneous phase discontinuities in the second harmonic.

The change in the $2Q_x$ harmonic spectral amplitudes were studied from a sextupole which was increased from $k_{2,\text{nom}}$ =

ISBN: 978-3-95450-184-7 doi:10.18429/JACoW-IPAC2018-THPAK137

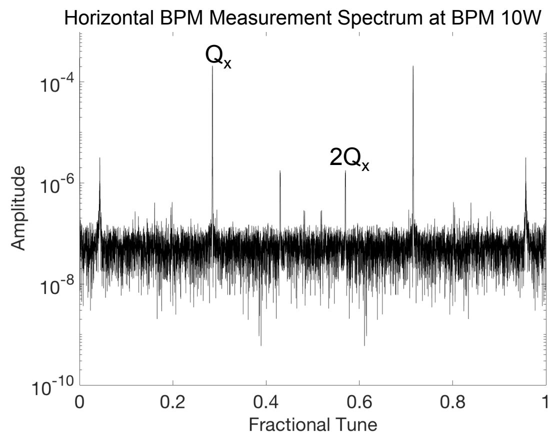

Figure 3: Example spectrum from experimental data collected at CESR, with nominal sextupole settings and one sextupole increase in field gradient. The fundamental harmonic and second harmonic spectral lines are labeled as Q_x and $2Q_x$ respectively.

0.56m^{-2} (where the "nom" the subscript on k_2 signifies the nominal settings) to $k_2 = 1.9k_{2,\text{nom}} = 1.04\text{m}^{-2}$ and then to $k_2 = 2.8k_{2,\text{nom}} = 1.56\text{m}^{-2}$ in two discrete steps. Figure 4 shows the measurement at each sextupole setting; it is clear that the amplitude scales linearly at each point. The inset histogram of the ratio between the amplitudes at each BPM shows that the distribution is highly peaked, and has a mean at 1.98. This ratio is a measurement of δk_2, because the nominal is subtracted, and the exact value of the ratio should therefore be 2.08, based on the readback value of the power supplies. A beam-based method for determining sextupole field gradients is precisely the tool needed in order to ensure these values are accurate, which our study hopes to provide as we continue our work.

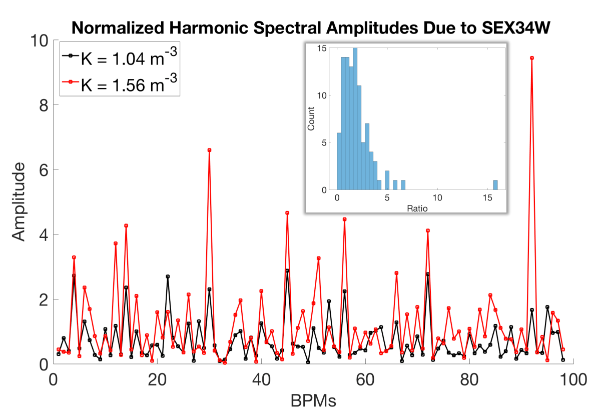

Figure 4: Second harmonic spectral line amplitudes for two increased sextupole field gradient settings, with inset displaying the distribution of the ratio of spectral line amplitude at each BPM. The ratio is highly peaked, with a mean of 1.98.

CONCLUSIONS AND FUTURE WORK

A simple model for CESR, in which there is a single sextupole and single BPM, was considered in order to develop a spectral analysis method for BPM measurements, which could be used to locate and measure sextupole field errors in the presence of tune jitter or initial offset. This model was shown to work in simulation, in which BPM measurements from a single sextupole left on the lattice were simulated, analyzed, and fit by the model. The fit located the sextupole element, and fit the field gradient K to within 0.5%. Experimental data have been collected to test the spectral analysis methods we developed. BPM measurements were collected at CESR in which the beam was resonantly driven by tune trackers, thus maintaining the phase of the beam excitation relative to the drive. The sextupoles were set to nominal settings which correct chromaticity, and a single sextupole gradient was increased in discrete steps. From the initial analysis, phase discontinuities have been observed in the linear and second harmonic phase advances, at the location following the increased sextupole. Further, the linear relationship between the amplitudes of the second harmonic spectral lines when the baseline has been removed, and the change in the field gradient has been observed. Further spectral analysis and use of the simple fitting model will continue, in order to develop a robust method for locating and measuring sextupole field gradients at CESR.

ACKNOWLEDGMENTS

This work was supported by NSF Award No. PHY-1549132 (Center for Bright Beams).

REFERENCES

[1] M. Billing, "The conversion of CESR to operate as the Test Accelerator, CesrTA", Part 1: overview, J. Instrum.,10(P07012)(2015).

[2] M. Borland 2013 J. Phys.: Conf. Ser. 425 042016.

[3] D. D. Caussyn, M. Ball, et al,. "Experimental studies of nonlinear beam dynamics", Phys. Rev. A 46, 7942 (1992).

[4] M. Giovannozzi, D. Quatraro, and G. Turchetti. "Generating unstable resonances for extraction schemes based on transverse splitting", Phys. Rev. ST Accel. Beams 12, 024003.

[5] A. Franchi, L. Farvacque, F. Ewald, G. Le Bec, & K. B. Scheidt. "First simultaneous measurement of sextupolar and octupolar resonance driving terms in a circular accelerator from turn-by-turn beam position monitor data", Phys. Rev. STAB, 17(074001)(2014).

[6] R. Tomas, "Normal form of particle motion under the influence of an ac dipole", PhysRevSTAB.5.054001.,(2002).

[7] M.G. Billing, J.A. Dobbins, M.J. Forster, D.L. Kreinick, R.E. Meller, M.C. Rendina, N.T. Rider, D.C. Sagan, J. Shanks, J.P. Sikora, M.G. Stedinger, C.R. Strohman, H.A. Williams, M.A. Palmer, R.L. Holtzapple, J. Flanagan. "Instrumentation for the study of low emittance tuning and beam dynamics at CESR", J. Instrum.,12 (T11006) (2017).

[8] D. Sagan, Bmad Reference Manual. http://www.lepp.cornell.edu/ dcs/bmad/.

ISBN: 978-3-95450-184-7 doi:10.18429/JACoW-IPAC2018-THPAK137

[9] M.G. Billing, W.F. Bergan, M.J. Forster, R.E. Meller, M.C. Rendina, N.T. Rider, D.C. Sagan, J. Shanks, J.P. Sikora, M.G. Stedinger, C.R. Strohman, M.A. Palmer, R.L. Holtzapple, "Beam position monitoring system at CESR", J. Instrum.,12(T09005)(2017).